Ab initio calculations of hyperfine structures of zinc and evaluation of the nuclear quadrupole moment $Q(^{67}\mathrm{Zn})$

Jacek Bieroń,[1,*] Livio Filippin,[2] Gediminas Gaigalas,[3] Michel Godefroid,[2] Per Jönsson,[4] and Pekka Pyykkö[5]

[1] *Instytut Fizyki imienia Mariana Smoluchowskiego, Uniwersytet Jagielloński, ul. prof. Stanisława Łojasiewicza 11, Kraków, Poland*

[2] *Chimie Quantique et Photophysique, Université libre de Bruxelles, B-1050, Brussels, Belgium*

[3] *Vilnius University, Institute of Theoretical Physics and Astronomy, Saulėtekio av. 3, LT-10222, Vilnius, Lithuania*

[4] *Department of Materials Science and Applied Mathematics, Malmö University, S-20506, Malmö, Sweden*

[5] *Department of Chemistry, University of Helsinki, PO Box 55 (A. I. Virtasen aukio 1), FIN-00014 Helsinki, Finland*

(Dated: April 2, 2018)

The relativistic multiconfiguration Dirac-Hartree-Fock (MCDHF) and the non-relativistic multiconfiguration Hartree-Fock (MCHF) methods have been employed to calculate the magnetic dipole and electric quadrupole hyperfine structure constants of zinc. The calculated electric field gradients for the $4s4p\ ^3P_1^o$ and $4s4p\ ^3P_2^o$ states, together with experimental values of the electric quadrupole hyperfine structure constants, made it possible to extract a nuclear electric quadrupole moment $Q(^{67}\mathrm{Zn}) = 0.122(10)$ b. The error bar has been evaluated in a quasi-statistical approach — the calculations had been carried out with eleven different methods, and then the error bar has been estimated from the differences between the results obtained with those methods.

PACS numbers: 31.15.A-, 31.30.Gs, 32.10.Fn, 21.10.Ky

I. INTRODUCTION

One of the most accurate methods to determine nuclear quadrupole moments, Q, is to combine measured nuclear quadrupole coupling constants, $B = e^2Qq/(4\pi\epsilon_0)h$ (in frequency units), with calculated or deduced electric field gradients (EFG), q [1]. The aim of the present work is to apply this method to determine improved nuclear quadrupole moments of zinc, the second most abundant essential trace element in the human body, after iron [2]. For zinc, the standard value cited in the 2008 review of Pyykkö [3] and the 2016 review of Stone [4] is still the 1969 value obtained by Laulainen and McDermott [5]: $Q(^{67}\mathrm{Zn}) = 0.150(15)$ b (1 barn = 1 b = $10^{-28}\,\mathrm{m}^2$). This value is based on the experimental $B_{63}(^3P_1^o) = -34.46(3)$ MHz for the $4s4p\,^3P_1^o$ state and a q value deduced from the experimental magnetic dipole hyperfine coupling constants $A_{67}(^3P_2^o) = 531.996(5)$ MHz [6] and $A_{67}(^3P_1^o) = 609.086(2)$ MHz [7]. The experimental ratio $B_{63}/B_{67} = 1.8347(13)$ of Laulainen and McDermott [5] corresponds to $Q(^{63}\mathrm{Zn}) = +0.275(30)$ b (incidentally, Laulainen and McDermott [5] arrived at $Q(^{63}\mathrm{Zn}) = +0.29(3)$ b). Potential improvements could be obtained by using the measurement of Byron *et al* [7] of $B(^3P_1^o) = -18.782(8)$ MHZ for the same $4s4p\,^3P_1^o$ state of ^{67}Zn. Their 65/67 ratio was $-0.1528(3)$ which, combined with their $Q(^{65}\mathrm{Zn})$ of 0.024(2) b, corresponds to $Q(^{67}\mathrm{Zn}) = 0.157$ b. More recently the EFGs of Zn in solid Zn have been calculated in a series of papers by Haas and collaborators [8–10], who employed the Density Functional Theory. In their latest paper [10] using a recently developed hybrid Density Functional Theory approach, combined with the experimental quadrupole coupling constants measured by Potzel *et al* [11], and corrected for thermal effects, they obtained a considerably smaller value of the quadrupole moment $Q(^{67}\mathrm{Zn}) = 0.125(5)$ b. The 5 mb error limit is considered as "may be optimistic" in the 2017 compilation of Pyykkö [12].

In the present work magnetic hyperfine interaction constants, A, and electric field gradients, q, necessary for an atomic evaluation of the quadrupole moments, were calculated for the $4s4p\ ^3P_1^o$ and $4s4p\ ^3P_2^o$ atomic states of the stable ^{67}Zn isotope using both the non-relativistic multiconfiguration Hartree-Fock (MCHF) method [13–15] and the fully relativistic multiconfiguration Dirac-Hartree-Fock (MCDHF) method [16–18]. MCHF is efficient in capturing electron correlation effects while MCDHF is necessary for correctly describing relativistic contraction due to the mass variation, influencing the wave function close to the nucleus. With this respect, the two methods were complementary: a 'DHF/HF factor' was used to correct the non-relativistic results for the relativistic effects and a 'triples correction' was used to correct the relativistic results for the electron correlation effects arising from triple substitutions, a calculation that became unfeasible in the fully relativistic scheme. The present work is the follow-up of the recent measurement of the hyperfine resonances of the $4s4p\,^3P_2^o \rightarrow 4s5s\,^3S_1$ transition by Wraith *et al* [19], as a detailed exposition of theoretical tools and computational approaches, employed to calculate magnetic fields and electric field gradients necessary for the evaluation of nuclear multipole moments.

The paper is divided into six sections. Section II introduces the essential elements of the multiconfiguration methods, as well as of the theory of the hyperfine struc-

* Jacek.Bieron@uj.edu.pl

ture in the non-relativistic and relativistic frameworks. Non-relativistic calculations are presented in section III, while section IV focuses on relativistic calculations. In section V we summarize the calculations, and we evaluate the nuclear quadrupole moment $Q(^{67}\mathrm{Zn})$ on the basis of eleven independent determinations of the electric field gradients. Section VI concludes the paper.

II. THEORY

A. Multiconfiguration methods

In multiconfiguration methods [15], the wave function, Ψ, for an atomic state is determined as an expansion over configuration state functions (CSFs)

$$\Psi = \sum_{i=1}^{N_{\mathrm{CSFs}}} c_i \Phi_i, \tag{1}$$

where N_{CSFs} is the number of CSFs in the expansion. The CSFs are coupled anti-symmetric products of one-electron orbitals. The expansion coefficients c_i and the radial parts of the one-electron orbitals are determined in a self-consistent procedure by finding stationary states of an energy functional based on a given Hamiltonian. Once a radial orbital set has been determined, configuration interaction (CI) calculations can be performed in which the expansion coefficients only are determined by diagonalizing the Hamiltonian matrix. CI calculations are simpler and faster than the self-consistent calculations and, for this reason, the number of CSFs can be extended.

Fully relativistic MCDHF calculations give wave functions for fine-structure states and are based on the Dirac-Coulomb Hamiltonian [16, 17]. The CSFs are obtained as jj-coupled and anti-symmetric products of Dirac-orbitals. The wave function representation in jj-coupling is transformed to an approximate representation in LSJ-coupling, using the methods and program developed by Gaigalas and co-workers [20, 21]. The non-relativistic MCHF calculations give wave functions for LS terms, and are based on the Schrödinger Hamiltonian [13, 15]. The CSFs are obtained as LS-coupled and anti-symmetric products of non-relativistic spin-orbitals.

The two methods have different strengths and weaknesses relative to the atomic system at hand. Zinc is a fairly relativistic system for which relativistic contraction due to the mass variation starts to get important, especially for the calculated hyperfine constants. These effects are captured very efficiently in the MCDHF method by the shape of the radial orbitals. Although the MCHF method corrected for relativistic effects through the Breit-Pauli approximation produces reliable atomic data for systems with relatively large nuclear charges [22], it will never fully account for these corrections at the level of orbital optimisation [23]. At the same time zinc is a large system with many subshells, and electron correlation effects captured by extended CSFs expansions are important for all computed properties. Due to the restriction to LS symmetry, the sizes of the CSF expansions for MCHF calculations grow less rapidly than do the corresponding expansions for the MCDHF calculations. As a consequence it is possible to include more electron correlation excitations in MCHF calculations.

B. Hyperfine structure

The hyperfine contribution to the Hamiltonian is represented by a multipole expansion

$$H_{\mathrm{hfs}} = \sum_{k\geq 1} \mathbf{T}^{(k)} \cdot \mathbf{M}^{(k)}, \tag{2}$$

where $\mathbf{T}^{(k)}$ and $\mathbf{M}^{(k)}$ are spherical tensor operators of rank k in the electronic and nuclear spaces. The $k = 1$ and $k = 2$ terms represent, respectively, the magnetic dipole (M1) and the electric quadrupole (E2) interactions. In non-relativistic calculations for an N-electron system the electronic contributions are obtained from the expectation values of the irreducible spherical tensors [24, 25]

$$\mathbf{T}^{(1)} = \frac{\alpha^2}{2} \sum_{j=1}^{N} \left\{ 2\mathbf{l}^{(1)}(j) \frac{1}{r_j^3} - g_s \sqrt{10} [\mathbf{C}^{(2)}(j) \times \mathbf{s}^{(1)}(j)]^{(1)} \frac{1}{r_j^3} + g_s \frac{8}{3} \pi \delta(\mathbf{r}_j) \mathbf{s}^{(1)}(j) \right\} , \tag{3}$$

and

$$\mathbf{T}^{(2)} = -\sum_{j=1}^{N} \mathbf{C}^{(2)}(j) \frac{1}{r_j^3} . \tag{4}$$

In the fully relativistic approach, the magnetic dipole electronic tensor reduces to a single term [26, 27]

$$\mathbf{T}^{(1)} = -i\alpha \sum_{j=1}^{N} \left(\boldsymbol{\alpha}_j \cdot \mathbf{l}_j \, \mathbf{C}^{(1)}(j) \right) \frac{1}{r_j^2} . \tag{5}$$

The electronic contribution for the magnetic dipole interaction is combined with the nuclear spin $I = 5/2$ and the measured nuclear magnetic dipole moment $\mu = 0.875479\,\mu_N$ [4] to give the magnetic dipole hyperfine interaction constant, A, for the $4s4p\,^3P^o_{1,2}$ states in ^{67}Zn. The electric field gradient (EFG), also denoted q [28], is obtained from the reduced matrix element of the operator (4) using the electronic wave function of the considered electronic state (see [27, 29] for details). It corresponds to the electronic part of the electric quadrupole hyperfine interaction constant, B. The latter, expressed in MHz, can be calculated using the following equation

$$B/\mathrm{MHz} \; = 234.9646\,(q/a_0^{-3})(Q/\mathrm{b})\;, \qquad (6)$$

where the EFG (q) and the nuclear quadrupole moment (Q) are expressed in a_0^{-3} and barns, respectively. Instead of reporting q, we will monitor in the present work the related $B/Q \propto q$ ratio values (in MHz/b).

III. NON-RELATIVISTIC CALCULATIONS

A. MCHF calculations

The MCHF calculations were performed using the Atomic Structure Package (ATSP2K) [30]. As a starting point a Hartree-Fock (HF) calculation was performed for $4s4p\,^3P^o$. The HF calculation was followed by a sequence of calculations describing valence-valence and core-valence electron correlation effects. The CSF expansions for these calculations were obtained by allowing single (S) and double (D) substitutions from $2s^22p^63s^23p^63d^{10}4s4p\,^3P^o$ to increasing active sets of orbitals with the restriction that there is at most one substitution from the core shells. The $1s$-shell is kept closed in all calculations. These expansions are referred to as all singles and restricted doubles (SrD) expansions. The active sets are denoted by giving the highest orbital of each symmetry. For example, $\{5s5p4d4f\}$ denotes the orbital set that includes the orbitals $1s, 2s, 3s, 4s, 5s, 2p, 3p, 4p, 5p, 3d, 4d, 4f$. In the MCHF calculations the HF orbitals were kept frozen and the remaining orbitals were optimized together. The MCHF calculations were followed by a CI calculation based on the largest orbital set. The CI calculation describes valence-valence (VV), core-valence (CV) and core-core (CC) correlation effects and includes CSFs obtained by all single and double (SD) substitutions. Whereas SD expansions describe the major corrections to the wave function, it is known that CSFs obtained from triple (T) substitutions are important for hyperfine structures [31]. The effects of the T substitutions were accounted for in CI, by augmenting the largest SD expansion with expansions obtained by T substitutions to increasing orbital sets. All calculations are summarized in Table I.

To correct for the relativistic contraction due to the mass variation, Dirac-Hartree-Fock (DHF) calculations were also performed and the final SD+T values were multiplied with the DHF/HF ratio. This correction will be discussed in more detail in the next section. From Table I we see that valence-valence and core-valence effects, as described by SrD expansions, increase the absolute values of all computed hyperfine parameters. The increase is around 30 % for the A constant and 60 % for the electric field gradient $q \propto B/Q$. The changes are well converged and are consistent with a contraction of the wave function when accounting for core-valence correlation as observed in [32, 33]. The effect of unrestricted D substitutions, resulting in CSFs describing also core-core correlation, is to decrease the absolute values of the computed hyperfine parameters. The CSFs resulting from the unrestricted double substitutions can be shown to have small effects on the hyperfine parameters by themselves. Instead the effects are indirect, changing or effectively diluting the mixing coefficients of the more important CSFs describing core-valence effects [34–37].

Finally, the effect of the T substitutions is to increase the absolute values of the hyperfine constants. Again, the effect is mainly indirect, affecting the expansion coefficients of the important singly excited CSFs: $2s^22p^63snl3p^63d^{10}4s4p\,^3P^o$ and $2snl2p^63s^23p^63d^{10}4s4p\,^3P^o$, describing spin-polarization; $2s^22p^63s^23p^5nl3d^{10}4s4p\,^3P^o$ and $2s^22p^5nl3s^23p^63d^{10}4s4p\,^3P^o$, the last two describing orbital-polarization [37, 38]. The latter effects will be analyzed in more detail in the section III C below. The general convergence trends and behavior with respect to different correlation effects are consistent with the ones found for other similar systems [36]. It is interesting to note that the effects discussed above are partly canceling. Thus it is better to include only the valence-valence and core-valence effects than the valence-valence, core-valence and core-core effects. If the core-core effects are included, then also the effects of the T substitutions should be accounted for. The final A constants for the $4s4p\,^3P^o_{1,2}$ states differ from the experimental values by 1.8 % and 5.2 %, respectively.

B. DHF/HF correction

Table II presents expectation values $\langle r\rangle_{nl}$ and $\langle r\rangle_{n\kappa}$ of spectroscopic orbitals obtained in zeroth-order (no electron correlation) non-relativistic Hartree-Fock (HF) and relativistic Dirac-Hartree-Fock (DHF) approximations, where $\kappa = -(l+1)$ for $j = l + 1/2$ and $\kappa = +l$ for $j = l - 1/2$. For all spectroscopic orbitals but $3d$, the direct relativistic contraction due to the mass variation dominates the indirect one, induced by the relativistic charge redistribution [39]. The differences in radii of correlation orbitals are more complex. They usually reflect specific correlation effects, targeted in the self-consistent-field optimisation strategies [15]. For the M1 hyperfine interaction, a detailed comparison of the non-relativistic expectation values of eq. (3) and of the relativistic ones

Table I. MCHF calculations of A (MHz) and B/Q (MHz/b) of $4s4p\ ^3P^o_{1,2}$ in ^{67}Zn ($I^\pi = 5/2^-$ and $\mu_{\rm expt} = 0.875479(9)\,\mu_N$). SrD denote all single and restricted double expansions to increasing active orbitals sets. SD denote single and double expansions to the largest orbital set. Single and restricted Double (SrD) expansions, with at most one substitution from the core shells, allow the inclusion of valence (VV) and core-valence (CV) effects (see text). Core-core correlation (CC) is included through unrestricted D substitutions. SD+T denote expansions where the largest SD expansion has been augmented by expansions from T substitutions to increasing active orbital sets. The largest SD+T results were scaled by the DHF/HF ratio factor in the line labeled MCHF×DHF/HF. HF = uncorrelated Hartree-Fock values; DHF = uncorrelated Dirac-Hartree-Fock values. $N_{\rm CSFs}$ is the number of CSFs in the expansion.

		$^3P^o_1$		$^3P^o_2$	
Label	$N_{\rm CSFs}$	A (MHz)	B/Q (MHz/b)	A (MHz)	B/Q (MHz/b)
HF		412.72451	−93.033	373.00296	186.066
DHF		473.40239	−100.373	419.93437	192.924
SrD (VV+CV)					
$5s5p4d4f$	404	471.978	−120.16	429.223	240.33
$6s6p5d5f5g$	1593	507.266	−136.52	459.667	273.04
$7s7p6d6f6g6h$	3872	526.518	−142.07	476.132	284.15
$8s8p7d7f7g7h$	7232	536.870	−146.85	484.970	293.70
$9s9p8d8f8g8h$	11673	541.017	−148.95	488.430	297.90
$10s10p9d9f9g9h$	17195	542.624	−148.27	489.789	296.55
$11s11p10d10f10g10h$	23798	542.926	−148.44	490.022	296.89
SD (VV+CV+CC)					
$11s11p10d10f10g10h$	44546	521.477	−137.738	470.799	275.476
SD+T (VV+CV+CC)					
$5s5p4d4f$	92810	533.150	−141.59	481.192	283.18
$6s6p5d5f5g$	225457	540.485	−144.86	487.481	289.73
$7s7p6d6f6g$	446457	544.960	−147.53	491.050	295.06
$8s8p7d7f7g$	761267	551.678	−151.68	496.389	303.36
$9s9p8d8f8g$	1175344	553.437	−152.988	497.691	305.976
MCHF × DHF/HF		634.802	−165.058	560.310	317.254
Expt.		609.086[a]		531.987[b]	

[a]Byron *et al* [7].
[b]Lurio [6].

of eq. (5) in terms of single-electron orbitals contributions is not easy. The global effect in the single configuration approximation is to produce large DHF/HF ratios of M1 and E2 hyperfine constants, as illustrated by the first two lines of Table I. As can be seen, the relativistic effect is much larger for the A constants than for the EFG values, which can be explained by the contact interaction that appears in the non-relativistic expression for the M1 interaction with the three-dimensional delta function (see the last term of eq. (3)). Although the corresponding relativistic expression of eq. (5) does not contain a contact operator, the tensorial structure of the relativistic operator indicates that it is highly biased towards the behavior of the wave function close to the nucleus where the relativistic contraction effects are the most important. Relativistic effects in nuclear quadrupole couplings have been investigated by Pyykkö and Seth [28] who estimated relativistic correction factors C for EFGs due to valence p electrons from one-electron matrix elements q_{++}, q_{+-} and q_{--}. The q_{--} combination has $j = 1/2$ for $l = 1$ and corresponds to a spherical charge distribution. It will therefore not contribute to the EFG, oppositely to q_{++} and q_{+-}. These C factors can be used to scale the non-relativistic EFG values. They have been estimated in the quasirelativistic (QR) approximation (no fine-structure splitting), using hydrogen-like (H) and Dirac-Fock (DF) expectation values, or the Casimir's n-independent formulae (Cas). They are reported in the first three lines of Table III. Beyond the QR approximation, correction factors can be estimated for the fine-structure levels of light atoms by taking the right combination of the C coefficients, $(-1/3\,C_{++} + 4/3\,C_{+-})$ and C_{++} for $J = 1$ and $J = 2$, respectively, with $C_{++} = 1.02556$ and $C_{+-} = 1.06177$ [28]. These factors are also reported in the Table III, and compared with the DHF/HF ratios estimated from the EFG values reported in Table I.

These ratios, obtained in the single configuration picture, may be used to scale the multiconfiguration results, as it is done in the line MCHF×DHF/HF of Table I, with the underlying assumption that cross terms between relativistic contraction and electron correlation are negligible. Looking at the differences in ratios between different methods, we infer that application of the DHF/HF corrective ratio induces an uncertainty of at most 2-3 % for the electric field gradient q of the $J = 1$ state. The un-

Table II. HF $\langle r\rangle_{nl}$ vs DHF $\langle r\rangle_{n\kappa}$ orbital radii (a_0). HF calculation for the $4s4p\ ^3P^o$ term. DHF calculation optimised on the $4s4p\ ^3P^o_{0,1,2}$ states together. Notation: 'nl' = HF orbital; '$nl+$' = DHF orbital with negative κ ($1s$, $2s$, $3s$, $4s$, $2p$, $3p$, $3d$, $4p$); 'nl$-$' = DHF orbital with positive κ ($2p-$, $3p-$, $3d-$, $4p-$). The table illustrates the direct relativistic contraction of s orbitals due to mass variation.

	$1s$	$2s$	$2p$	$3s$	$3p$	$3d$	$4s$	$4p$
nl	0.05108	0.22878	0.19951	0.69107	0.71948	0.87132	2.77730	3.80035
$nl+$	0.05028	0.22498	0.19912	0.68097	0.71824	0.87909	2.72995	3.79473
$nl-$			0.19578		0.70820	0.87169		3.76246

certainty is smaller for the $J = 2$ state.

C. Contributions to A and EFG from different classes of orbital substitutions

The uncertainties of the computed A constants and electric field gradients q are to a large extent determined by the size of the cancellation effects [40, 41]. In the non-relativistic formalism the A constants are computed based on the operator in eq. (3) and are the sums of three terms A_l, A_{sd}, A_c, orbital, spin-dipolar, and Fermi contact term, respectively. At the HF level we have (in MHz): $A_l = 33.06$, $A_{sd} = 33.10$, $A_c = 346.56$, and $A_l = 33.06$, $A_{sd} = -6.62$, $A_c = 346.56$, for $4s4p\,^3P^o_1$ and $4s4p\,^3P^o_2$, respectively. It is seen that the Fermi contact term dominates, but this contribution is partly canceled by the spin-dipolar contribution for the $J = 2$ state. Based on this simple observation we may expect that the computed A constant is less accurate for the $J = 2$ state. To shed light on the sensitivity of A and B/Q to electron correlation effects we analyze the contributions to these parameters from different classes of orbital substitutions. Given the $\{11s11p10d10f10g10h\}$ orbital set, the A constants and B/Q ratio values are computed from accumulated CSF expansions that result from allowing single and double substitutions from deeper and deeper lying orbitals of the $2s^22p^63s^23p^63d^{10}4s4p$ reference configuration. The results are presented in Table IV. The accumulated CSF expansions are denoted by the innermost orbitals from which the substitutions are allowed. For example, $3d3d$ denotes the accumulated CSF expansion that is obtained by allowing the substitutions

$$vv \rightarrow nln'l',\ 3dv \rightarrow nln'l',\ 3d \rightarrow nl,\ 3d3d \rightarrow nln'l'$$

whereas $3pv$ denotes the accumulated CSF expansion obtained from the substitutions

$$\begin{gathered} vv \rightarrow nln'l' \\ 3dv \rightarrow nln'l' \\ 3d \rightarrow nl \\ 3d3d \rightarrow nln'l' \\ 3pv \rightarrow nln'l' \end{gathered}$$

where nl, $n'l' \in \{11s11p10d10f10g10h\}$. By comparing the results for $3d3d$ and $3pv$ we can infer how large are the contributions from CSFs obtained from the $3pv \rightarrow nln'l'$ substitutions. From Table IV one can see that CSFs obtained from $3dv \rightarrow nln'l'$ substitutions describing core-valence correlation are very important for both A and B/Q. One can also see that CSFs obtained from $3s$, $2s \rightarrow nl$ substitutions describing spin-polarization are important for the A parameters whereas CSFs obtained from $3d$, $3p$, $2p \rightarrow nl$ substitutions describing orbital-polarization are important for the q parameters. One further notes that the effects of CSFs from single substitutions are often canceled by those of CSFs from double substitutions. Of particular importance are the effects from $3d3d \rightarrow nln'l'$. The corresponding CSFs do not directly contribute to the hyperfine parameters but they are important for the total wave function, lowering, or diluting, the effects of the other CSFs (compare the discussion in the previous section). The accuracy of the calculated A constant and (B/Q) ratio values is to a large extent determined by the fact that they result from a summation of a number of canceling contributions. We refer to chapter 8 of [14] for a general discussion about spin- and orbital-polarization effects.

IV. MULTICONFIGURATION DIRAC-HARTREE-FOCK/RCI CALCULATIONS

Two different approaches were used for the $4s4p\ ^3P^o_{1,2}$ states. In the first approach, called OL1 (Optimal Level 1) the wave functions for the $4s4p\ ^3P^o_2$ state were optimised for a single state, i.e. the $4s4p\ ^3P^o_2$ level itself. In the second approach (called OL4) the wave functions were generated with the Extended Optimal Level [42] form of the variational functional, built from all 4 states of the $4s4p$ configuration ($4s4p\ ^3P^o_0$, $^3P^o_1$, $^3P^o_2$, $^1P^o_1$). The full description of numerical methods, virtual orbital sets, electron substitutions, and other details of the computations, can be found in [15, 18, 29, 43–46].

A. Optimal Level calculations for the $4s4p\,^3P^o_2$ state

As mentioned above, the first approach (OL1) targets the optimisation of the single state $4s4p\ ^3P^o_2$ wave function. The spectroscopic orbitals $1s2sp3spd4sp$ were generated in Dirac-Hartree-Fock (DHF) mode, i.e. without correlation (virtual) orbitals, and were frozen through all further steps. Five layers of virtual orbitals [45] of s,p,d,f,g,h angular symmetries were sequentially gener-

Table III. Relativistic correction factors for EFG estimated with different methods. Quasirelativistic correction factors reported are taken from Ref. [28] using Dirac-Fock (DF), Hydrogen-like (H) expectation values or the Casimir's n-independent formulae (Cas) (see Ref. [28] for more details.) The J-dependent correction factors are either calculated following the procedure outlined in the conclusion section of Ref. [28], or from the DHF/HF ratio of EFG values (this work). "+" = $p_{3/2}$ orbital; "−" = $p_{1/2}$ orbital.

QR approach	1.05468	$C_{\rm QR}$(Cas) : Casimir's n-independent formula [28]
	1.05776	$C_{\rm QR}$(H) : H-like [28]
	1.04970	$C_{\rm QR}$(DF) : DHF [28]
$J = 1$	1.07384	calculated from [28] $(-1/3\,C_{++} + 4/3\,C_{+-})$
	1.07890	DHF/HF ratio, this work (1st line of Table I).
$J = 2$	1.02556	calculated from [28] (C_{++})
	1.03686	DHF/HF ratio, this work (2nd line of Table I).

Table IV. The effect on A and B/Q ($\propto$ EFG) of $4s4p\ ^3P^o_{1,2}$ from different classes of orbital substitutions. Analysis for the final SD calculation. See text for details of the notation and for a discussion about the importance of different classes.

	$^3P^o_1$		$^3P^o_2$	
Label	A (MHz)	B/Q (MHz/b)	A (MHz)	B/Q (MHz/b)
HF	412.72	−93.033	373.00	186.06
vv	411.07	−92.28	371.67	184.56
$3dv$	479.96	−109.23	433.48	218.46
$3d$	479.93	−112.88	434.33	225.76
$3d3d$	459.77	−106.35	416.60	212.71
$3pv$	470.26	−109.49	425.92	218.98
$3p3d$	469.76	−109.55	425.52	219.10
$3p$	477.31	−133.89	428.89	267.78
$3p3p$	475.54	−133.21	427.30	266.43
$3sv$	478.39	−133.58	429.93	267.16
$3s3d$	479.19	−133.96	430.54	267.92
$3s3p$	479.35	−134.17	430.60	268.34
$3s$	506.62	−134.16	457.86	268.32
$3s3s$	506.11	−134.07	457.38	268.15
$2pv$	509.65	−135.20	460.48	270.40
$2p3d$	509.88	−135.52	460.61	271.05
$2p3p$	509.72	−135.34	460.47	270.68
$2p3s$	509.71	−135.44	460.41	270.89
$2p$	512.05	−139.21	461.24	278.43
$2p2p$	509.03	−137.95	458.45	275.90
$2sv$	510.21	−138.12	459.55	276.25
$2s3d$	510.53	−138.08	459.86	276.16
$2s3p$	510.91	−138.08	460.24	276.16
$2s3s$	511.00	−138.06	460.33	276.13
$2s2p$	511.36	−138.15	460.66	276.30
$2s$	521.91	−137.89	471.20	275.78
$2s2s$	521.47	−137.73	470.79	275.47

ated by including single and double substitutions (SD) for the first two layers and single and restricted double substitutions (SrD) for the third, fourth, and fifth layer.

The occupied shells were successively opened for substitutions into virtual set, starting with $4sp$, followed by $3spd$, and then by $2sp$. The $1s$ shell was kept closed in all calculations. The multiconfiguration self-consistent-field optimisation step was followed by configuration interaction (RCI) calculations, in which CSF expansions were appended with configurations arising from subsets of unrestricted single and double (SD) substitutions, or with (subsets of) unrestricted single, double, and triple (SDT) substitutions.

Figure 1 shows the dependence of the magnetic dipole hyperfine constant A (MHz), (curves in the upper graph of the figure), and the B/Q ratio (MHz/b), proportional to EFG, of the $4s4p\ ^3P^o_2$ state (curves in the lower graph of the figure), on the size of the multiconfiguration expansion. All lines in both graphs are drawn only for the guidance of the eyes. The results of the calculations are represented by several symbols described in the following paragraph. Each integer value on the abscissa axis represents the maximal principal quantum number of the virtual orbital set for a particular multiconfiguration expansion. The fractional values represent approximations, where CSF expansions were appended with subsets of SD or SDT expansions. In these configuration interaction calculations, these subsets were generated in the following ways: the occupied orbitals were systematically opened for SD and SDT substitutions; the size of the virtual orbital set was systematically increased for SD substitutions, until the expectation values saturated with respect to the size of the virtual orbital set; then the size of the virtual orbital set was systematically increased for SDT substitutions. The convergence of the SDT results was not reached since larger SDT multiconfiguration expansions would exceed the capacity of the computer systems at our disposal (6x96 CPU @ 2.4GHz with 6x256 GB RAM).

A stepwise, systematic increase of different classes of substitutions makes it possible to identify those classes which bring about considerable contributions to the expectation value(s), as well as to quantify these contributions. Those with sizeable contributions were later included in the final configuration interaction calculations. Four curves in Figure 1 represent the following correlation models:

- circles (black online) = single and restricted double substitutions (SrD);
- squares (green online) = unrestricted single and double (SD) substitutions;

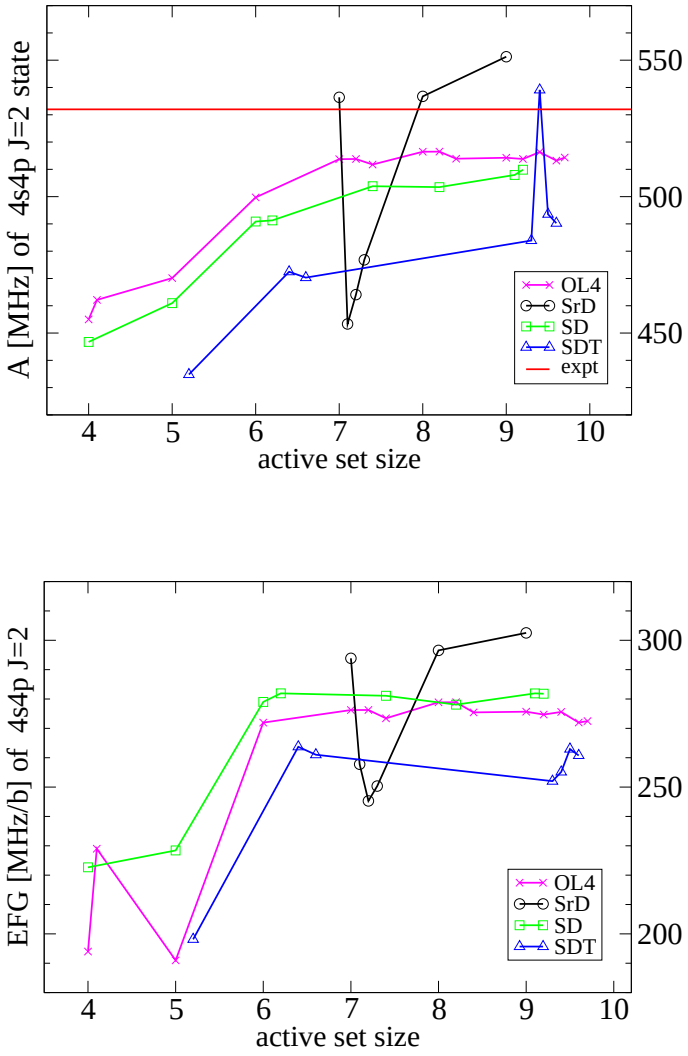

Figure 1. (Color online) Hyperfine constant $A(4s4p\ ^3P_2^o)$ (MHz) (curves in the upper graph of the figure) and B/Q ratio (MHz/b) of the $4s4p\ ^3P_2^o$ state (curves in the lower graph of the figure), obtained in several approximations. Each integer value on the abscissa axis represents the maximal principal quantum number of the virtual orbital set for a particular multiconfiguration expansion. The fractional values represent approximations, where multiconfiguration expansions were appended with subsets of SD or SDT expansions. The straight horizontal line (red online) represents the experimental value $A(^3P_2^o) = 531.987(5)$ MHz. More details are provided in text.

- triangles (blue online) = single and double and triple (SDT) substitutions;
- crosses (magenta online) = results of the OL4 calculation, described in section IV C below.

The curves with circles (black online) represent the initial phase of the calculations, where the third, fourth, and fifth layers of virtual orbitals were generated with single and restricted double substitutions (SrD). These results were not corrected for unrestricted double (SD), nor for triple (SDT) substitutions. The curves with triangles (blue online) represent the configuration interaction calculations, where unrestricted double and triple (SDT) substitutions were included. However, due to the limitations of available computer resources the triple substitutions were limited to substitutions from $4s$,$4p$ occupied orbitals to one layer of virtual orbitals, or substitutions from $3s$,$3p$,$3d$,$4s$,$4p$ occupied orbitals to two layers of virtual orbitals. The oscillations of the blue curves is a clear evidence that the triple substitutions were not saturated in these calculations.

The SD and OL4 curves, with squares (green online) and crosses (magenta online) in both upper and lower graphs, respectively, in Figure 1 represent the values corrected for the triple substitutions in a systematic manner: the triple substitutions were accounted for with an additive correction computed with the non-relativistic Hartree-Fock program ATSP2K [30] (see section IV B below).

The straight horizontal line (red online) accross the upper part of the upper graph in Figure 1 represents the experimental magnetic dipole hyperfine constant $A = 531.987(5)$ MHz for the $4s4p\ ^3P_2^o$ state of the ^{67}Zn isotope [6].

The end products of the calculations described in the present section are the magnetic dipole hyperfine constant, $A = 509.861$ MHz and the $B/Q = 281.799$ MHz/b ratio represented in Figure 1 by the points at the right hand side ends of the curve with squares (green online) on the upper and lower graphs, respectively. These values were obtained from the configuration interaction calculation with single and double substitutions from $2sp3spd4sp$ occupied orbitals to five layers of virtual orbitals (the largest size of the virtual orbital set generated in this approximation). These results, corrected for triple substitutions as described in the section IV B below, were considered final in the single-reference calculations described in the present section. They are quoted in Table IX in line marked 'MCDHF-SD-SR-OL1+t(MCHF)'.

The scatter of points at the right hand side end of the four curves presented in the Figure 1 and the oscillations of the individual curves could serve as a guideline for estimating the error bars of the theoretical EFG contribution to B, and indirectly to $Q \propto B/q$. In the present paper however, the error bars have been estimated with a somewhat more reliable procedure described in the section V below.

B. Additive corrections for triple substitutions

If the contribution of triple substitutions is small, it may be approximately assumed as an additive correction, approximately independent of relativity, and may be computed in the non-relativistic framework as the difference between the values obtained with and without triple substitutions, respectively. As an example, the correction (31.96 MHz) for the magnetic dipole hyperfine constant $A(4s4p\ ^3P_1^o)$ in Table V was evaluated as

Table V. Corrections for triple substitutions, (SDT−SD), calculated for hyperfine constant A (MHz) and B/Q (MHz/b) in $4s4p\ ^3P^o_{1,2}$ states.

	$A(J=1)$	$B/Q(J=1)$	$A(J=2)$	$B/Q(J=2)$
SD	521.4771	-137.7380	470.7987	275.4760
SD+T	553.4370	-152.9882	497.6906	305.9764
SDT−SD	31.96	-15.25	26.89	30.50

the difference between the value calculated in the SD+T approximation (A = 553.4370 MHz) and the value calculated in the SD approximation (A = 521.4771 MHz). Analogous differences were assumed as triple contributions for the $A(4s4p\ ^3P^o_2)$ constant, as well as for the B/Q ratio-values for both states.

C. Extended Optimal Level calculations for the $4s4p\,^3P^o_1$ and $4s4p\,^3P^o_2$ states

The calculations described in this section were performed in a similar manner as those presented in section IV A, with one significant difference: wave functions were optimised for all four states of $4s4p$ configuration ($4s4p\ ^3P^o_0$, $^3P^o_1$, $^3P^o_2$, $^1P^o_1$) in the Extended Optimal Level (OL4) approach [42], with equal weights. The calculations of hyperfine A and EFG factors for $4s4p\ ^3P^o_{1,2}$ states presented in this section are computationally more demanding than those for $4s4p\ ^3P^o_2$ state presented in section IV A. The $4s4p$ configuration splits into four levels ($^3P^o_0$, $^3P^o_1$, $^3P^o_2$, $^1P^o_1$) and there are two levels of $J = 1$ symmetry. The singlet $^1P^o_1$ state interacts considerably with the triplet $^3P^o_1$ state, and in such situations optimisation on all close lying levels often yields a better balance of states involved in configuration mixings. However, the multiconfiguration expansions are larger, and self-consistent-field process requires considerably more computer resources. The end products of the calculations described in the present section are the hyperfine A constants and B/Q ratios for the $4s4p\ ^3P^o_{1,2}$ states, obtained from the configuration interaction calculation with single and double substitutions from $2sp3spd4sp$ occupied orbitals to five layers of virtual orbitals (the largest size of the virtual orbital set generated in this approximation). These results, corrected for triple substitutions as described in the section IV B above, were considered final in the Extended Optimal Level calculations and they are quoted in Table IX in lines marked 'MCDHF-SD-SR-OL4+t(MCHF)' (separately for $4s4p\ ^3P^o_1$ state and $4s4p\ ^3P^o_2$ state). The results of these calculations for the $4s4p\ ^3P^o_2$ state are also represented by (magenta online) curves with crosses in Figure 1.

D. Liu *et al*'s approach

Other computation strategies have been attempted and it is worthwhile to test their coherence. Liu *et al* [47] focused on the spin-forbidden transition $4s^2\ ^1S_0 - 4s4p\ ^3P^o_1$ and the hyperfine-induced transition $4s^2\ ^1S_0 - 4s4p\ ^3P^o_0$ for ions between Z = 30 (Zn) and Z = 47 (Ag). These authors considered the following active set sequence

$$\begin{aligned}
\text{AS1} &= \{4s, 4p, 4d, 4f\},\\
\text{AS2} &= \text{AS1} + \{5s, 5p, 5d, 5f, 5g\},\\
\text{AS3} &= \text{AS2} + \{6s, 6p, 6d, 6f, 6g\},\\
\text{AS4} &= \text{AS3} + \{7s, 7p, 7d, 7f, 7g\},\\
\text{AS5} &= \text{AS4} + \{8s, 8p, 8d, 8f, 8g\}.
\end{aligned} \tag{7}$$

Their electron correlation model took into account the VV correlation, CV correlation through excitations of maximum one core electron from the $3d$, $3p$ and $3s$ subshells, as well as spin-polarization (SP) effects by including CSFs of the forms $1s^22s^22p^63s(ns)3p^63d^{10}$, $1s^22s(ns)2p^63s^23p^63d^{10}$ and $1s(ns)2s^22p^63s^23p^63d^{10}$. CC correlation was systematically neglected. The A and B values that they obtained for the $4s4p\ ^3P^o_1$ level of ^{67}Zn are respectively A = 20.21 mK and B = −0.7539 mK, to be compared with the two experimental results A = 20.317(7) mK (609.086(2) MHz) and B = −0.6265(3) mK (−18.782(8) MHz) from Byron *et al* [7]. The corresponding results are denoted as MCDHF-SrDT-SP-Liu.

E. Wave functions optimised for isotope shifts

Relativistic MCDHF wave functions have been recently optimised for estimating the electronic isotope shift parameters of $4s^2\ ^1S_0 - 4s4p\ ^3P^o_1$ and $4s4p\ ^3P^o_2 - 4s5s\ ^3S_1$ by Filippin *et al* [48]. Oppositely to hyperfine parameters, a reliable calculation of transition isotope shifts requires a correct balance of electron correlation effects between the levels involved. These authors attempted three different strategies, systematically omitting core-core correlation in the variational process of orbital optimisation. It is indeed well-known that CC correlation effects are better balanced with the use of a common orbital basis for describing both states involved in a given transition. Neglecting CC enables to get separate orbital basis sets to allow orbital relaxation. It is interesting to investigate the hyperfine constants calculated with these computational strategies. In the present work, we estimate the hyperfine structure parameters using three approaches labelled hereafter M1, M2 and M3.

The first approach (M1) was inspired by the strategy of Liu *et al* [47], also omitting core-core correlation. Single (S) and double (D) substitutions were performed

Table VI. A (MHz), B/Q (MHz/b), and Q (b) values calculated with method M1 (see section IV E), as functions of the increasing active space for the $4s4p\,^3P_1^o$ and $4s4p\,^3P_2^o$ states in ^{67}Zn I, $I^\pi = 5/2^-$ and $\mu_{\rm expt} = 0.875479(9)\,\mu_N$. The Q-values are extracted from the relation $Q = B_{\rm expt}/(B/Q)$, where the experimental values are $B_{\rm expt}(^3P_1^o) = -18.782(8)$[a] MHz and $B_{\rm expt}(^3P_2^o) = 35.806(5)$[b] MHz.

	$4s4p\,^3P_1^o$				$4s4p\,^3P_2^o$			
Active space	$N_{\rm CSFs}$	A (MHz)	B/Q (MHz/b)	Q (b)	$N_{\rm CSFs}$	A (MHz)	B/Q (MHz/b)	Q (b)
MCDHF-SrDT-SP (VV+CV)								
$5s5p4d4f$	1 592	558.02	−131.036	0.1433	2 122	483.71	254.975	0.1404
$6s6p5d5f5g$	11 932	590.45	−146.084	0.1286	16 961	507.74	280.708	0.1276
$7s7p6d6f6g6h$	48 574	610.80	−150.997	0.1244	71 610	529.87	290.233	0.1234
$8s8p7d7f7g7h$	128 264	613.17	−152.617	0.1231	191 495	532.46	292.535	0.1220
$9s9p8d8f8g8h$	267 998	617.02	−154.391	0.1217	402 586	536.97	296.441	0.1208
$10s10p9d9f9g9h$	484 772	618.47	−154.071	0.1219	730 853	537.48	294.773	0.1215
Liu *et al* [47]		605.9	−150.7	0.1247				
Expt.		609.086(2)[a]				531.987(5)[b]		

[a]Byron *et al* [7].
[b]Lurio [6].

on a single-reference (SR) set. These SD-SR substitutions take into account valence-valence (VV) and core-valence (CV) correlations. A VV correlation model only allows SD substitutions from valence orbitals, while the VV+CV correlation model considers SrDT substitutions (single plus restricted double and triple) from core and valence orbitals, limiting the substitutions to a maximum of one hole in the core. *Separate* orbital basis sets were optimised for the two studied states $^3P_{1,2}^o$. One difference with respect to the procedure reported in [48] for isotope shift parameters is that the $1s$ shell is opened in the present work to include the spin-polarisation effects that are relevant for hyperfine structure calculations. The procedure can be outlined as follows:

(1) Perform a calculation using a set consisting of CSFs with two forms: $[\mathrm{Ar}]3d^9nln'l'n''l''\,J^\Pi$ and $[\mathrm{Ne}]3s^23p^53d^{10}nln'l'n''l''\,J^\Pi$ with $n, n', n'' = 4$ and $l, l', l'' = s, p, d, f$, plus $5s$ and $5p$. These CSFs account for a fair amount of the VV correlation, and for CV correlations between the $3p$ and $3d$ core orbitals and the $5s$, $5p$ and $n = 4$ valence orbitals. Add spin polarisation (SP) by including the following CSFs:
$1s^22s^22p^63s3p^63d^{10}4s4p5s\,J^\Pi$,
$1s^22s2p^63s^23p^63d^{10}4s4p5s\,J^\Pi$,
$1s2s^22p^63s^23p^63d^{10}4s4p5s\,J^\Pi$.

(2) Keep the orbitals fixed from step (1), and optimise an orbital basis, layer by layer, up to an active space equal to $10s10p9d9f9g9h$, described by CSFs with the J^Π symmetry of the state. These CSFs are obtained by SrDT-SP substitutions as in step (1) (at most one substitution from the $1s^22s^22p^63s^23p^63d^{10}$ core [49]).

The corresponding results are presented in Table VI. The MCDHF-SrDT-SP-Liu active space expansion used in [47] optimised simultaneously the $^3P_1^o$ and $^3P_2^o$ levels. Therefore the A, B/Q and Q results obtained in the present work slightly differ from those reported in [47] for $J = 1$.

The second approach (M2) considered single and restricted double substitutions performed on a single-reference (SR) set (MCDHF-SrD-SR). The VV correlation model only allows SD substitutions from valence orbitals, while the VV+CV correlation model considers SrD substitutions from core and valence orbitals, limiting the substitutions to a maximum of one hole in the core. Oppositely to Filippin *et al* [48], core correlation is included in the final step through a configuration interaction calculation based on SD-SR expansions. The corrections for triple excitations estimated in section IV B (see Table V), are added in the very final step. This computational strategy can be outlined by the following sequence:

(1) Run a calculation using SR set consisting of CSF(s) of the form $2s^22p^63s^23p^63d^{10}4s4p\,J^\Pi$.

(2) Keep the orbitals fixed from step (1), and optimise an orbital basis layer by layer up to an active space equal to $11s11p10d10f10g10h$, described by CSFs with the J^Π symmetry of the state. These CSFs are obtained by SrD-SR substitutions (at most one substitution from the $2s^22p^63s^23p^63d^{10}$ core).

(3) Perform a CI calculation on the CSFs expansion with the J^Π symmetry of the state, describing VV, CV and CC correlation obtained by SD-SR substitutions to the orbital basis from step (2).

(4) Add a correction to the A and EFG values from step (3), accounting for triple (t) substitutions and obtained from a non-relativistic MCHF computation.

Step (3), allowing the inclusion of core-core correlation through CI, and step (4), specific to hyperfine constants, were not considered in [48]. The corresponding results are denoted MCDHF-SrD-SR/CI-SD-SR+t(MCHF) in

Table VII. MR configurations for the $4s4p\,^3P_1^o$ and $4s4p\,^3P_2^o$ states in ^{67}Zn I. The MR-cutoff value, $\varepsilon_{\rm MR}$, determines the set of CSFs in the MR space. $N_{\rm CSFs}$ is the number of CSFs describing each MR space.

State	$\varepsilon_{\rm MR}$	MR configurations	$N_{\rm CSFs}$
$4s4p\,^3P_1^o$	0.01	$[{\rm Ar}]3d^{10}\{4s4p, 4p4d\},\ [{\rm Ar}]3d^9\{4s4p4d, 4s4d4f, 4p^3, 4p^24f, 4s^24p\}$	31
$4s4p\,^3P_2^o$	0.01	$[{\rm Ar}]3d^{10}\{4s4p, 4p4d\},\ [{\rm Ar}]3d^9\{4s4p4d, 4s4d4f, 4p^3, 4p^24f, 4s^24p\}$	31

Table VIII. A (MHz), B/Q (MHz/b), and Q (b) values calculated with methods M2 (upper part) and M3 (lower part) - see section IV E), as functions of the increasing active space for the $4s4p\,^3P_1^o$ and $4s4p\,^3P_2^o$ states in ^{67}Zn I. $I^\pi = 5/2^-$ and $\mu_{\rm expt} = 0.875479(9)\,\mu_N$. The Q-values are extracted from the relation $Q = B_{\rm expt}/{\rm EFG}$, where the experimental values are $B_{\rm expt}(^3P_1^o) = -18.782(8)$[a] MHz and $B_{\rm expt}(^3P_2^o) = 35.806(5)$[b] MHz.

	$4s4p\,^3P_1^o$				$4s4p\,^3P_2^o$			
Active space	$N_{\rm CSFs}$	A (MHz)	B/Q (MHz/b)	Q (b)	$N_{\rm CSFs}$	A (MHz)	B/Q (MHz/b)	Q (b)
$4s4p3d$ (DHF)	2	475.27	−100.437	0.1870	1	419.98	192.166	0.1863
MCDHF-SrD-SR (VV+CV)								
$5s5p4d4f$	1 454	554.21	−129.614	0.1449	2 108	483.74	253.875	0.1410
$6s6p5d5f5g$	5 857	590.45	−145.650	0.1290	5 790	509.32	280.362	0.1277
$7s7p6d6f6g6h$	14 381	617.54	−152.198	0.1234	14 467	534.86	292.975	0.1222
$8s8p7d7f7g7h$	27 052	627.21	−157.702	0.1191	27 426	542.93	303.008	0.1182
$9s9p8d8f8g8h$	43 870	627.36	−159.448	0.1178	44 667	547.10	305.735	0.1171
$10s10p9d9f9g9h$	64 835	631.06	−159.859	0.1175	66 190	550.27	306.528	0.1168
$11s11p10d10f10g10h$	89 947	632.63	−159.987	0.1174	91 995	550.84	306.521	0.1168
+ $1s$ open	95 907	638.82	−159.974	0.1174	97 610	556.64	306.592	0.1168
CI-SD-SR (VV+CV+CC)								
$11s11p10d10f10g10h$	1 236 101	546.09	−129.845	0.1446	1 243 611	479.14	249.303	0.1436
+ t(MCHF) $9s9p8d8f8g$		578.05	−145.095	0.1294		506.03	279.803	0.1280
Multireference calculations								
$5s5p4d4f$ (MR)	903	541.40	−112.267	0.1673	1 231	414.61	198.252	0.1806
MCDHF-SrD-MR (VV+CV)								
$6s6p5d5f5g$	12 015	595.05	−148.023	0.1269	16 521	511.98	284.444	0.1259
$7s7p6d6f6g6h$	32 172	621.07	−153.354	0.1225	45 722	535.07	294.919	0.1214
$8s8p7d7f7g7h$	62 730	631.14	−159.206	0.1180	90 401	544.19	306.010	0.1170
$9s9p8d8f8g8h$	103 689	630.28	−160.573	0.1170	150 558	548.36	308.353	0.1161
$10s10p9d9f9g9h$	155 049	633.80	−160.991	0.1167	226 193	551.29	309.010	0.1159
$11s11p10d10f10g10h$	216 810	635.32	−161.006	0.1167	317 306	551.96	308.985	0.1159
+ $1s$ open	232 787	641.60	−161.025	0.1167	339 230	557.60	309.005	0.1159
Expt.		609.086(2)[a]				531.987(5)[b]		

[a] Byron *et al* [7].
[b] Lurio [6].

the upper part of Table VIII. The final line shows that opening $1s$ brings a non-negligible contribution to the A-values, which become approximately 6 MHz larger for both states. This approach is very similar to the method described in section IV A. However, the advantage of the M2 calculations is in the simultaneous generation of both $4s4p\ ^3P_2^o$ and $4s4p\ ^3P_1^o$ states, at the Optimal Level (OL) of the variational functional. For $4s4p\ ^3P_2^o$, the results are indeed very similar to the MCDHF-SD-SR-OL1+t(MCHF) values already reported in Table IX and discussed in section IV A dedicated to that level. For these M2 results, only the $4s4p\ ^3P_1^o$ values are therefore reported in the final summary in Table IX.

The third approach (M3) considered SrD substitutions performed on a multi-reference (MR) set. The latter contains the CSFs that have large expansion coefficients and account for the major correlation effects. For building this MR set, a MCDHF calculation is first performed using a CSF expansion based on SrDT substitutions from the $3d$ and the occupied valence orbitals towards the $5s$, $5p$ and $n = 4$ valence orbitals (maximum of one hole in the $3d$ orbital).

Due to limited computer resources, such an MR set would be too large for subsequent calculations. Hence, only the CSFs whose expansion coefficients are, in absolute value, larger than a given MR cutoff are kept, i.e., $|c_\nu| > \varepsilon_{\rm MR}$. The resulting MR sets are outlined in Table VII. Only orbitals occupied in the single configuration DHF approximation are treated as spectroscopic, and the occupied reference orbitals are kept frozen in the subsequent calculations.

The M3 procedure consists in the following sequence:

(1) Perform a calculation using an MR set consisting of CSFs with two forms:
$2s^22p^63s^23p^63d^{10}nln'l'\,J^\Pi$ with $n, n' = 4$ and $l, l' = s, p, d, f + 5s$ and $5p$, and
$2s^22p^63s^23p^63d^9nln'l'n''l''\,J^\Pi$ with $n, n', n'' = 4$ and $l, l', l'' = s, p, d, f + 5s$ and $5p$. These CSFs account for a fair amount of the VV correlation, and for CV correlations between the $3d$ core orbital and the $5s$, $5p$ and $n = 4$ valence orbitals. Keep in the MR set the CSF whose expansion coefficients are, in absolute value, larger than $\epsilon_{\rm MR} = 0.01$.

(2) Keep the orbitals fixed from step (1), and optimise an orbital basis layer by layer up to an active space equal to $11s11p10d10f10g10h$, described by CSFs with the J^Π symmetry of the state. These CSFs are obtained by SrD-MR substitutions (at most one substitution from the $2s^22p^63s^23p^63d^{10}$ core). As observed for M2, spin-polarisation of the $1s$ shell is not negligible. The results of these calculations are presented in the lower part of Table VIII, and labeled MCDHF-SrD-MR in Table IX.

V. EVALUATION OF THE NUCLEAR QUADRUPOLE MOMENT OF $Q(^{67}\mathrm{Zn})$

Table IX. Summary of the A (MHz), B/Q (MHz/b) , and Q (b) values of ^{67}Zn.

State	A (MHz)	B/Q (MHz/b)	Q (b)	Method
$4s4p\ ^3P_1^o$	634.802	−165.058	0.113790	MCHF-SD(T)
	605.9	−150.7	0.1247	MCDHF-SrDT-SP-Liu
	618.47	−154.071	0.121905	MCDHF-SrDT-SP
	641.60	−161.025	0.116640	MCDHF-SrD-MR
	578.05	−145.095	0.129446	MCDHF-SrD-SR/CI-SD-SR+t(MCHF)
	577.886	−142.579	0.131730	MCDHF-SD-SR-OL4+t(MCHF)
	609.086(2)[a]			Expt.
$4s4p\ ^3P_2^o$	560.310	317.254	0.112862	MCHF-SD(T)
	537.48	294.773	0.121470	MCDHF-SrDT-SP
	557.60	309.005	0.115875	MCDHF-SrD-MR
	509.861	281.799	0.127062	MCDHF-SD-SR-OL1+t(MCHF)
	513.200	271.989	0.131645	MCDHF-SD-SR-OL4+t(MCHF)
	531.987[b]			Expt.

[a] Byron *et al* [7].
[b] Lurio [6].

We report in the present section eleven calculated Q (and A) values, obtained with the following approaches:

- MCHF-SD/CI-SDT+DHF/HF correction ($^3P^o_{1,2}$ levels), under label MCHF-SD(T), - see sections III A and III B,
- MCDHF-SrDT-SP-Liu: from Liu *et al* [47] (only $^3P^o_1$ level), - see section IV D,
- MCDHF-SrDT-SP: calculation based on Liu *et al*'s strategy ($^3P^o_{1,2}$ levels) - see method M1 in section IV E,
- MCDHF-SrD-SR/CI-SD-SR+t(MCHF): single-reference + MCHF triples correction ($^3P^o_1$ level [50]) - see method M2 in section IV E,
- MCDHF-SrD-MR: multi-reference ($^3P^o_{1,2}$ levels), - see method M3 in section IV E,
- MCDHF-SD-OL1+t(MCHF): OL1 ($J = 2$) single reference + MCHF triples correction (only $^3P^o_2$ level) - see section IV A,
- MCDHF-SD-OL4+t(MCHF): OL4 ($J = 0, 1, 1, 2$) single reference + MCHF triples correction ($^3P^o_{1,2}$ levels) - see section IV C,

where the shorthand notations above represent the following computational methods:

MCHF	MultiConfiguration Hartree-Fock (non-relativistic)
CI-SDT	Configuration Interaction Hartree-Fock (non-relativistic)
DHF/HF	multiplicative relativistic correction described in section III
MCDHF	MultiConfiguration Dirac-Hartree-Fock (relativistic)
SD	Single and Double substitutions in the SCF process
SrD	Single and restricted Double substitutions in the SCF process
t(MCHF)	additive correction for triple substitutions estimated from MCHF calculation (see section IV B).
SP	Spin Polarisation (method described in Liu *et al* [47])
SR	Single-Reference
MR	Multi-Reference
OL1	Optimal Level calculation with optimisation on one level (J=2)
OL4	Optimal Level calculation with optimisation on four levels

We adopted a convention used by chemists, where T in parentheses (T) implies that triple substitutions are included in a post-SCF approach (Møller-Plesset or CI or another method). In our notation t(MCHF) means an additive correction for triple substitutions evaluated with the ATSP code [30]. The calculated EFGs were combined with the measured B values for the $4s4p\ ^3P^o_1$ state [7], and for the $4s4p\ ^3P^o_2$ state [6] of the neutral Zn atom, to yield eleven calculated values of $Q(^{67}\mathrm{Zn})$, presented in the fourth column of Table IX.

Although these eleven values do not represent the sample in the statistical sense, the scatter of the values gives us an information about the dependence of the calculated values of EFG on the choice of the method of calculation, and provides a basis for an estimate of the error bar for the determination of the quadrupole moment $Q(^{67}\mathrm{Zn})$. We assumed that the error bar should at least overlap with all eleven results. For computing the final value of $Q(^{67}\mathrm{Zn})$ one might consider taking the average of the results of the eleven calculations ($Q = 0.1208$ b), or the median value thereof ($Q = 0.1223$ b); both methods yield very close results, the difference being negligible compared to the error bar resulting from the arguments presented above. Assuming the above procedures and estimates, we arrived at $Q(^{67}\mathrm{Zn}) = 0.12 \pm 0.01$ b, obtained from the $4s4p\ ^3P^o_{1,2}$ states of zinc. The relative error bar (8 %) is of the same order as the error bar (10 %) associated with the previous standard value, $Q(^{67}\mathrm{Zn}) = 0.150(0.015)$ b, quoted by Stone [4] and by Pyykkö [3], and based on measurements performed by Laulainen and McDermott [5], but the $Q(^{67}\mathrm{Zn})$ value itself is now downshifted by 20 %. On the other hand, our value is in very good agreement with $Q(^{67}\mathrm{Zn}) = 0.125(5)$ b, of Haas *et al* [10], who used a hybrid Density Functional Theory approach.

An inspection of the results presented in the Table IX leads to the conclusions, that the multi-reference MCDHF-SrD-MR calculations overshoot the values of the magnetic dipole hyperfine constant A by about $20 - 25$ MHz, while single reference MCDHF-SD-SR-OL1+t(MCHF) and MCDHF-SD-SR-OL4+t(MCHF) results for A are too small by nearly the same amount. The best agreement with the experimental A value was obtained in the calculation of Liu *et al* [47], which is understandable, since, as mentioned in section IV D, the main objective of Liu *et al* was the magnetic dipole hyperfine structure, therefore they carefully treated the spin-polarization effects. Incidentally, the nuclear quadrupole moment $Q(^{67}\mathrm{Zn})$ calculated from their EFG value is in fact quite close to the median value $Q = 0.1223$ b, mentioned above. The abovementioned discrepancies may be assumed as another tool to estimate the error bar for determination of Q. The error bar estimate from A is of the order of 4 %, smaller than that obtained from the sample of eleven Q values. We assumed the larger of the two error bar estimates, and finally we propose

$$Q(^{67}\mathrm{Zn}) = 0.122(10)\ \mathrm{b}\ . \tag{8}$$

This value has been utilized to extract electric quadrupole moments of odd-A nuclei in the range $A = 63$–79 across the isotopic chain of zinc, following the measurements of electromagnetic moments by Wraith *et al* [19].

VI. CONCLUSIONS

The calculations of hyperfine shifts are inherently inaccurate (or accurate to a few percent). We do have computational tools to estimate accuracy of expectation values [29, 44, 45], but they are more expensive computationally than the calculations of expectation values themselves. Therefore we rarely *compute* accuracy, because normally we compute the expectation values themselves at the limits of our computing resources, and this does not leave enough resources for computing accuracy. Then we *estimate* the accuracy. Estimating the accuracy of a single calculation of an EFG for a single level is in fact not much more than guesswork. If magnetic dipole hyperfine coupling constant A is known (i.e. measured A_{expt} exists) then accuracy of EFG is sometimes assumed from the difference $A_{\mathrm{expt}} - A_{\mathrm{calc}}$. Another method is to carry out calculations with several different methods and evaluate the accuracy from differences between the results obtained with those methods. In the present paper the

latter approach yields the larger error bar. The optimal method would be to carry out measurements and calculations for several levels. From this point of view having hyperfine structure data for several levels would give us a benefit of more tools to estimate accuracy. Combined with measured values of A and B for these levels, we would obtain a *statistical* sample for both A and EFG. It is not exactly statistical because calculations are in principle not fully independent, but several levels is still better than one or two levels.

ACKNOWLEDGMENTS

The large-scale calculations were carried out with the supercomputer Deszno purchased thanks to the financial support of the European Regional Development Fund in the framework of the Polish Innovation Economy Operational Program (contract no. POIG.02.01.00-12-023/08). Computational resources have also been provided by the Shared ICT Services Centre, Université libre de Bruxelles and by the Consortium des Équipements de Calcul Intensif (CÉCI), funded by the Fonds de la Recherche Scientifique de Belgique (F.R.S.-FNRS) under Grant No. 2.5020.11. MG was supported by the Belgian F.R.S.-FNRS Fonds de la Recherche Scientifique (CDR J.0047.16) and FWO & FNRS Excellence of Science Programme (EOS-O022818F). This work is also supported by the Swedish Research Council under contract 2015-04842.

[1] P. Pyykkö, Mol. Phys **99**, 1617 (2001).
[2] F. H. Nielsen, in *Handbook of Nutrition and Food*, edited by C. D. Berdanier, J. T. Dwyer, and D. Heber (CRC Press, 2013) pp. 211–226.
[3] P. Pyykkö, Mol. Phys **106**, 1965 (2008).
[4] N. J. Stone, At. Data Nucl. Data Tables **111-112**, 1 (2016).
[5] N. S. Laulainen and M. N. McDermott, Phys. Rev. **177**, 1606 (1969).
[6] A. Lurio, Phys. Rev. **126**, 1768 (1962).
[7] J. F. W. Byron, M. N. McDermott, R. Novick, B. W. Perry, and E. B. Saloman, Phys. Rev. **134**, A47 (1964).
[8] H. Haas and J. G. Correia, Hyperfine Interact. **198**, 133 (2010).
[9] H. Haas, M. B. Barbosa, and J. G. Correia, Hyperfine Interact. **237**, 115 (2016).
[10] H. Haas, S. P. A. Sauer, L. Hemmingsen, V. Kellö, and P. W. Zhao, Europhys. Lett. **117**, 62001 (2017).
[11] W. Potzel, T. Obenhuber, A. Forster, and G. M. .Kalvius, Hyperfine Interact. **12**, 135 (1982).
[12] P. Pyykkö, Molecular Physics **000**, 000 (2018), doi: 10.1080/00268976.2018.1426131.
[13] C. Froese Fischer, *The Hartree-Fock Method for Atoms: A numerical approach* (J. Wiley & Sons, New York, 1977).
[14] C. Froese Fischer, T. Brage, and P. Jönsson, *Computational Atomic Structure. An MCHF Approach* (Institute of Physics Publishing, Bristol and Philadelphia, 1997).
[15] C. Froese Fischer, M. Godefroid, T. Brage, P. Jönsson, and G. Gaigalas, J. Phys. B: At. Mol. Opt. Phys. **49**, 182004 (2016).
[16] I. P. Grant, Comput. Phys. Commun. **84**, 59 (1994).
[17] I. P. Grant, *Relativistic Quantum Theory of Atoms and Molecules: Theory and Computation* (Springer, New York, 2007).
[18] P. Jönsson, G. Gaigalas, J. Bieroń, C. Froese Fischer, and I. P. Grant, Comput. Phys. Commun. **184**, 2197 (2013).
[19] C. Wraith, X. F. Yang, L. Xie, C. Babcock, J. Bieroń, J. Billowes, M. Bissell, K. Blaum, B. Cheal, L. Filippin, R. Garcia Ruiz, W. Gins, L. Grob, G. Gaigalas, M. Godefroid, C. Gorges, H. Heylen, M. Honma, P. Jönsson, S. Kaufmann, M. Kowalska, J. Krämer, S. Malbrunot-Ettenauer, R. Neugart, G. Neyens, W. Nörtershäuser, F. Nowacki, T. Otsuka, J. Papuga, R. Sánchez, Y. Tsunoda, and D. T. Yordanov, Phys. Lett. B **771**, 385 (2017).
[20] G. Gaigalas, T. Žalandauskas, and Z. Rudzikas, At. Data Nucl. Data Tables **84**, 99 (2003).
[21] G. Gaigalas, C. Froese Fischer, P. Rynkun, and P. Jönsson, Atoms **5**, 1 (2017).
[22] C. Froese Fischer, G. Tachiev, and A. Irimia, At. Data Nucl. Data Tables **92**, 607 (2006).
[23] M. Godefroid, P. Jönsson, and C. Froese Fischer, Phys. Scr. **T78**, 33 (1998).
[24] A. Hibbert, Rep. Prog. Phys. **38**, 1217 (1975).
[25] P. Jönsson, C.-G. Wahlström, and C. Froese Fischer, Comput. Phys. Commun. **74**, 399 (1993).
[26] I. Lindgren and A. Rosén, Case Stud. At. Phys. **4**, 93 (1974).
[27] P. Jönsson, F. Parpia, and C. Froese Fischer, Comput. Phys. Commun. **96**, 301 (1996).
[28] P. Pyykkö and M. Seth, Theor. Chem. Acc. **96**, 92 (1997).
[29] J. Bieroń, C. Froese Fischer, S. Fritzsche, G. Gaigalas, I. P. Grant, P. Indelicato, P. Jönsson, and P. Pyykkö, Phys. Scr. **90**, 054011 (2015).
[30] C. Froese Fischer, G. Tachiev, G. Gaigalas, and M. Godefroid, Comput. Phys. Commun. **176**, 559 (2007).
[31] S. G. Porsev and A. Derevianko, Phys. Rev. A **73**, 012501 (2006).
[32] I. Lindgren, J. Lindgren, and A.-M. Mårtensson, Z. Phys. A: Hadrons Nucl. **279**, 113 (1976), 10.1007/BF01437866.
[33] S. Salomonson, Z. Phys. A: At. Nucl. **316**, 135 (1984).
[34] B. Engels, Theor. Chim. Acta **86**, 429 (1993).
[35] B. Engels, L. A. Eriksson, and S. Lunell, Adv. At. Mol. Phys. **27**, 297 (1996).

[36] P. Jönsson, A. Ynnerman, C. Froese Fischer, M. R. Godefroid, and J. Olsen, Phys. Rev. A **53**, 4021 (1996).
[37] M. Godefroid, G. Van Meulebeke, P. Jönsson, and C. Froese Fischer, Z. Phys. D: At. Mol. Clusters **42**, 193 (1997).
[38] B. Engels, S. Peyerimhoff, and E. Davidson, Mol. Phys. **62**, 109 (1987).
[39] J.-P. Desclaux, in *Relativistic Electronic Structure Theory. Part 1. Fundamentals.*, edited by P. Schwerdtfeger (Elsevier, 2002) p. 1.
[40] T. Carette and M. R. Godefroid, Phys. Rev. A **83**, 062505 (2011).
[41] T. Carette and M. R. Godefroid, J. Phys. B: At. Mol. Opt. Phys. **44**, 105001 (2011).
[42] K. G. Dyall, I. P. Grant, C. T. Johnson, F. A. Parpia, and E. P. Plummer, Comput. Phys. Commun. **55**, 425 (1989).
[43] J. Bieroń, C. Froese Fischer, and I. P. Grant, Phys. Rev. A **59**, 4295 (1999).
[44] J. Bieroń, P. Jönsson, and C. Froese Fischer, Phys. Rev. A **60**, 3547 (1999).
[45] J. Bieroń, C. Froese Fischer, P. Indelicato, P. Jönsson, and P. Pyykkö, Phys. Rev. A **79**, 052502 (2009).
[46] P. Jönsson and J. Bieroń, J. Phys. B: At. Mol. Opt. Phys. **43**, 074023 (2010).
[47] Y. Liu, R. Hutton, Y. Zou, M. Andersson, and T. Brage, J. Phys. B: At. Mol. Opt. Phys. **39**, 3147 (2006).
[48] L. Filippin, J. Bieroń, G. Gaigalas, M. Godefroid, and P. Jönsson, Phys. Rev. A **96**, 042502 (2017).
[49] The original notation adopted in [48] was (SrDT-SS) where the 'SS' stands for "single s substitutions" describing spin-polarisation (SP) of the core s subshells.
[50] The corresponding $^3P_2{}^o$ results are not reported in Table IX since the strategy is similar to the MCDHF-SD-OL1+t(MCHF) method (see section IV A), with consistent results.